ISSN XXXX XXXX © 2017 IJESC

Research Article Volume 7 Issue No.11

A comprehensive Parametric Study of the Effect of Cavitation Formation Inside Fuel Injector Nozzle with Different Needle Seat Shapes

Sepideh Amirahmadian
Master
Department of Mechanical Engineering
Islamic Azad University South Branch of Tehran, Iran

Abstract:
In this work, fluid flow inside three liquid fuel injector nozzles was simulated numerically using Ansys-Fluent v16 commercial code. A mixture model along with the k-ε turbulence model was used to handle the two-phase and turbulent nature of this flow. The Schnerr-Sauer model was used to model the cavitation phenomena. After validation of the present numerical scheme using Winklhofer rectangular shape nozzle, a real size four-hole injector nozzle was used to investigate in detail the effects of pressure difference, cavitation number and needle height on the flow pattern. It was found that with increase of the cavitation number the cavitation length increases. The results indicate that for the case with larger needle height, the vapor volume fraction inside the injector nozzles is significantly larger. It was also concluded that increasing the cavitation number and needle height can increase discharge coefficient until occurrence of a fully cavitating field inside the injector. In the second part of the present study; VCO (Valve-Covered-Orifice), improved and standard injector nozzle with different seat shapes were simulated in order to investigate the effect of the valve seat shape on the cavitation phenomena. Numerical simulation also shows that in all three injector nozzles that have been computationally analyzed in this work, increasing the cavitation number can increase the discharge coefficient, but for the injector with standard seat shape, the discharge coefficient has smaller value in comparison with the other two injector nozzles. In addition, flow separation area due to the low pressure field is much larger in the standard nozzle compared to VCO nozzle and the improved nozzle. Under similar boundary conditions, the standard nozzle has larger vapor volume fraction length than in case of two other nozzles, while the vapor volume fraction region for the improved nozzle is much shorter. Lastly, formation of turbulent intensity along the orifice of the three aforementioned nozzles is highly different. The turbulent intensity for standard nozzle is larger compared with the two other nozzles. Therefore, it can be pointed out that although standard nozzle has lower discharge coefficient compared to the two other nozzles analyzed, the higher value of turbulent intensity and vapor volume fraction for this type of nozzle shows that air-fuel mixtures have better quality in this injector nozzle than in two other nozzles considered in this analysis.

Keywords: Cavitation, Diesel Injector, Simulation

1. INTRODUCTION

Flow pattern inside internal nozzle flow can have strong impact on spray and it's atomization [1-5]. Since 1892, diesel engines, has always been an integral part of propulsion and energy for higher thermal efficiency [6-8]. Cavitation, inside nozzle plays an important part on the internal flow in diesel injector nozzles [9-12]. In high pressure, previously, a research team lead by Wei Shyy [13, 14] presented excellent analytical modeling, numerical simulations and verification against experimental results for external cavitating flows. Zeidi and Mahdi [3-6] investigated cavitation inside rectangular shape nozzle of Winklhofer nozzle that has rectangular cross section by utilizing Ansys Fluent v14 software and by developing an Eulerian-Lagrangian analysis code. Using Eulerian-Lagrangian code, they calculated forces acting on the surface of the bubble and concluded that added mass force is much higher than other five forces acting on the bubble's surface especially in the direction of gravity. Singhal cavitation model [15] was used in their paper to calculate the effect of several parameters including the effects of contraction inside nozzle's orifice, effect of compressibility, nozzle contraction, and orifice entry for low pressure nozzle. It was found that increasing contraction will decrease maximum outlet velocity of the nozzle. The effect of compressibility of vapor phase in a rectangular shape nozzle can also increase discharge coefficient. They also found that increasing viscosity can decrease velocity of fluid in the near wall region [16-17]. Salvador et al. [18] studied cavitation phenomena inside nozzle by acquisition of numerical methods under different degrees of needle lift. It was found that under different degree of needle lift, formation of cavitation phenomena and mass flow rate inside nozzle will change greatly. Molina et al. [19] was able to compare flow and cavitation phenomena inside the oval and round nozzles by using numerical modeling method. It was found that inside oval nozzle discharge coefficient is very low and possibility of cavitation occurrence is not high; on the other hand, for round nozzle cavitation can be occurred much easing and also discharge coefficient was reported much higher. Wang and Su [20] investigated the unstable cavitation phenomena due to pressure fluctuation inside the nozzle and it was found that due to local pressure and flow rate, occurrence of cavitation phenomena will be delayed. Sun et al. [21] by acquisition of semi steady method for investigation of cavitation phenomena inside nozzle, could find factors that can effect mass flow rate and fuel injection. Salvador et al. [22, 23] by comparing cavitation phenomena inside microsac and VCO nozzle, could find that various nozzle and nozzle chamber can

highly affect cavitation. Most two different approaches is used to perform cavitation modelling: Continuum model and two fluid model [24–27]. In continuum model, vapor and liquid are treated as homogenous, while, two fluid model considers liquid and vapor separately. In the mentioned two models, pressure and velocity are related together with an equation of state for calculating cavitation growth. Forty plain different orifices was measured by Ohrn et al. [28]. It was found that discharge coefficient can significantly be affected by condition of nozzle inlet, in which Reynolds number and length diameter ration where not affected that much. Kato et al. [29] by measuring discharge hole and distribution of pressure in a sac nozzle could find that cavitation phenomena is affected by both inlet whole geometry and nozzle sac geometry. Payri et al. [30, 31] found that cavitation phenomena can increase speed of flow at the outlet and also spray cone angle can be increased. Bergstrand [32] after comparing five different nozzle for five different hole shapes, it was found that lower fuel consumption and lower emissions can be achieved in lower fuel rate. Sibendu Som et al. [33] investigated hydro-grinding and whole conicity on combustion processes and spray by coupling spray simulation and injector flow. It was found that hydor-grinding and conicity can decrease turbulence and cavitation inside nozzle that can augment spray penetration. In this paper, cavitation inside real size 3D fuel injection nozzles will be investigated. A comprehensive comparison of performance among nozzles having different seat shapes will also be performed.

2. GOVERNING EQUATION

For simulating flow inside injector nozzle, the model was created inside Gambit and afterward flow inside injector nozzle is modelled using Ansys Fluent software. Due to using computation fluid dynamic model and significant effect of mesh topology on the final result, investigating mesh dependency is very important. In this study, two phase flow is modelled with single fluid model (homogenous mixture). Continuity and momentum equations are as following:

$$\frac{\partial}{\partial t}(\rho_m) + \nabla.(\rho_m \vec{v}_m) = 0 \quad (1)$$

$$\frac{\partial}{\partial t}(\rho_m) + \nabla.(\rho_m \vec{v}_m.\vec{v}_m) = -\nabla p + \nabla.[\mu_m(\nabla\vec{v}_m + \nabla\vec{v}_m^T)] + \rho_m\vec{g} \quad (2)$$

$\vec{v}_m$ is velocity vector for homogenous flow, ρ_m is density of mixture and μ_m is viscosity of mixture which are as following:

$$\rho_m = \alpha_l\rho_l + \alpha_v\rho_v \quad (3)$$

$$\mu_m = \alpha_l\mu_l + \alpha_v\rho_v \quad (4)$$

α is vapor volume fraction for each phase. α_v is vapor volume fraction for vapor phase and α_l is vapor volume fraction for liquid phase. If we assume radius of bubble as R_B, α_v can be calculated as following:

$$\alpha_v = \frac{n_b\frac{4}{3}\pi R_B^3}{1+n_b\frac{4}{3}\pi R_B^3} \quad (5)$$

In equation (5), n_b is number of bubbles in a unit of volume.
For calculating mass transfer from liquid to vapor, Schnerr and Sauer Cavitation model is used [34]. The mentioned equation for vapor volume fraction has the following general shape:

$$\frac{\partial}{\partial t}(\alpha_v.\rho_v) + \nabla.(\alpha_v.\rho_v.V_v) = \frac{\rho_v.\rho_l}{\rho}.\frac{d\alpha_v}{dt} \quad (6)$$

Also source term can be calculated as following:

$$R = \frac{\rho_v\rho_l}{\rho}\frac{d\alpha_v}{dt} \quad (7)$$

For linkage between numbers of vapor volume fraction of bubbles in a unit volume of liquid, the following equation is used:

$$R = \frac{\rho_v\rho_l}{\rho}\alpha_v(1-\alpha_v)\frac{3}{R_B}\sqrt{\frac{2}{3}\frac{(P_v-P)}{\rho_l}} \quad (8)$$

Radius of bubble can be calculated from the following equation:

$$R_B = \left(\frac{\alpha_v}{1-\alpha_v}\frac{3}{4\pi}\frac{1}{n_b}\right)^{\frac{1}{3}} \quad (9)$$

Mostly discharge coefficient and cavitation number are introduced for defining flow inside diesel injector nozzle when cavitation occurs. Discharge coefficient is ratio of real mass flow rate to ideal mass flow, which can be calculated form Bernoulli equation:

$$Cd = \frac{\dot{m}}{A\sqrt{2\rho_l(P_{in}-P_{back})}} \quad (10)$$

$\dot{m}$ is real mass flow rate and A is cross sectional area of the nozzle. Cavitation number can be defined as following:

$$K = \frac{P_{in}-P_v}{P_{in}-P_{back}} \quad (11)$$

In which P_v is vaporization pressure, P_{in} is inlet pressure and P_{back} is back pressure. The mathematical derivation used by Zeidi et al. [35-38] is also used in this study and the current quality of calculation is increasing by used the mentioned procedure.

3.VALIDATION

In order to validate result that was obtained from Ansys-Fluent, at first rectangular shape nozzle from Winklhofer et al. [34] in which experimental data is available was modeled in Gambit and simulated in Ansys-Fluent. Figure 1a shows Winklhofer rectangular cross section shape nozzle in which the geometry is specified. Moreover, in figure 2a, mesh for Winklhofer rectangular shape nozzle is demonstrated in which hexahedral mesh is dominant. Figure 2 also shows variation of mass flow rate versus pressure in which Winklhofer experimental data was also used to validate current numerical procedure. As figure 2 shows, current numerical solution can predict mass flow very well in cavitation inception (pressure difference is 60 bar), super cavitation (pressure difference is 75 bar) and choke condition (pressure difference is 80 bar). From figure 2, it can also be inferred that mass flow rate in choke condition will not change, so that the current numerical method can be predict it. $k-\varepsilon$ turbulent model was used since it had lower discrepancy for the current study in comparison with $k-\omega$.

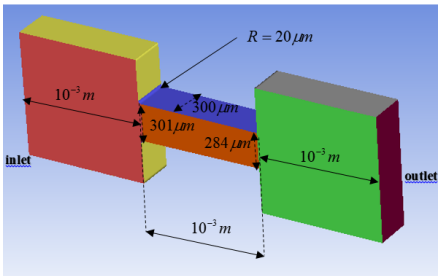

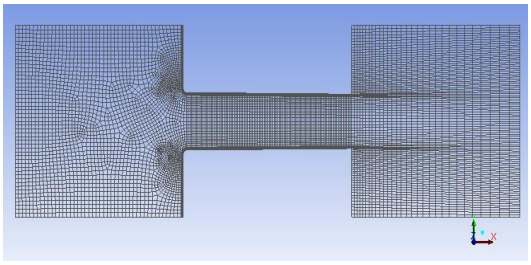

a) b)

Figure 1. Winklhofer rectangular cross section shape nozzle

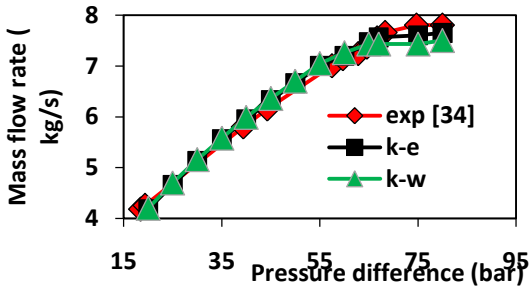

Figure 2. Variation of mass flow rate versus pressure difference

Figure 3 also shows formation of vapor volume fraction for cavitation inception ($\Delta P = 6\,MPa$) and super cavitation ($\Delta P = 2.5\,MPa$). As this figure shows at lower pressure difference formation of vapor volume fraction is trivial, while increasing pressure difference can cause super cavitation to occur.

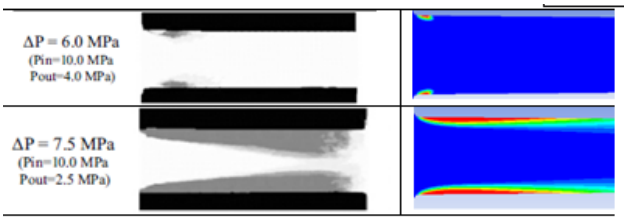

Figure 3. Vapor volume fraction for cavitation inception and super cavitation

Table 1 show the boundary condition which was used in the current study. In this table inlet and outlet boundary conditions which was used in this is utilized in order to investigate the flow inside nozzle. Also material properties such as density, viscosity and surface tension are mentioned in table 1. Cavitation parameters have also been mentioned in table 1. According to table 1, inlet pressure is $10\,MPa$ and outlet pressure varies from $1\,MPa$ to $6\,MPa$. Material properties which was suggested by Darvish et al. [39- 43] and Kadkhodapour and Raeisi [44], has been very helpful to find the following properties which are very critical to estimate for appropriate simulation.

Table.1. Initial boundary condition for the current simulation

		Diesel fuel (liquid)	Diesel fuel (vapor)
physical properties	density (kg/m^3)	840	0/029
	viscosity (kg/m.s)	0/0025	$3/1\times10^{-6}$
	surface tension (N/m)	0/02	-
	vaporization pressure (pa)	870	-
Initial boundary condition	Pressure inlet		10 Mpa
	Pressure outlet		1-6 Mpa
	Turbulence intensity		$0.16 \times Re^{-1/8}$
	Turbulence length scale		0.07D
Cavitation Parameters	Cavitation model		Schnerr-Sauer
	Number of bubble per unit of volume (m^{-3})	$n_b = n_{ref} \times \left((p_v - p)/p_v\right)^{2/2}$	
	Critical pressure in cavitation (Pa)	$p_{cr} = p_v + 2\mu(1 + C_t\mu_t/\mu) \times S_{max}$	

4. GEOMETRY OF FOUR HOLE REAL SIZE NOZZLE

Figure 4 shows geometry of four-hole injector nozzle. As this figure shows for reducing calculation cost only one-fourth of the nozzle is modeled and instead of that periodic boundary condition is used. Also in figure 4, pressure inlet and pressure outlet are clarified. A mesh of 245600 cells was used in this part of the current study. Figure 5 shows length of the orifice area beside inlet and outlet radius of orifice area. Moreover, needle height is also shown in this figure. Figure 5 shows important dimensions for modeling nozzle. Diameter of orifice is $0.32\,mm$ and length of orifice is $1.3\,mm$. Injector has a needle which control mass flow rate as it goes up and down. The distance between needle surface and chamber is shown with h in figure 5. The nozzle which is shown in figure 5 is standard nozzle and as needle goes down, mass flow rate decreases and flow which enters to orifice will decrease. Standard nozzle has a sac region in which orifice hole is located in it. In this study as it is shown in figure 4, structured mesh is used.

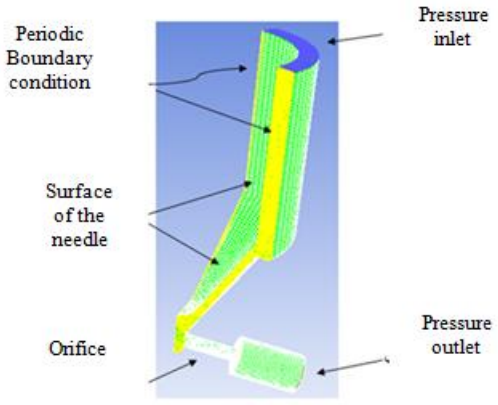

Figure.4. Geometry of four-hole injector nozzle

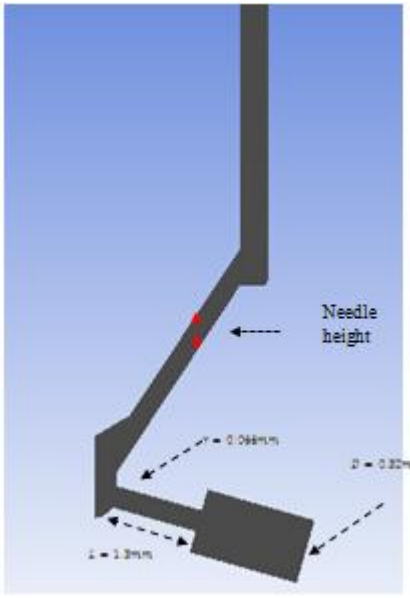

Figure .5. Dimensions of real size nozzle

5. RESULT AND DISCUSSION

In this study, by changing inlet pressure and needle height different simulations are done. $k-\varepsilon$ turbulence model which has been previously used by Hamedi et al and Ketabdar and Hamedi [45-48] and validated by experimental results [49-51] is used with wall functions. SIMPLE algorithm has also been used for pressure and velocity linkage. Shnerr and Sauer cavitation model is used to evaluate cavitation phenomena in the current study. Number of bubble in a unit volume of liquid, n_b, is an important parameter in simulating the flow inside nozzle. Most this parameter is evaluated experimentally. For the current nozzle n_b was calculated for water previously; therefore carrying fluid in this part of study is water.

Table 2. Thermodynamic properties of water

Carrying fluid	water
Density (kg/m^3)	998
Viscosity (Ns/m^2)	0/001
Vaporization pressure (Pa)	2360
Temperature (K)	293
Number of bubble in unit volume of liquid	$1/9 \times 10^{11}$

By fixing outlet pressure of nozzle, inlet pressure should change according to cavitation number in the simulations in this study. Injector height changes from maximum value which is $h = 0.54\,mm$ to minimum value which is $h = 0.04\,mm$. For each needle height relevant simulations is also performed.
Figure 6 shows velocity distribution in mid-plane of the nozzle $\boldsymbol{h = 0.1mm}$ and $\boldsymbol{k^{0.5} = 1.094}$. When flow enters to orifice, due to sudden decrease in cross sectional area, velocity of flow increases, while decreasing static pressure causes the phase to change and cavitation will form. Since the flow is stagnant in the sac region and acts like obstacle in front of flow, there for incoming flow in the upper part of orifice is much more and decreasing value of static pressure is more probable; hence, occurrence of cavitation can be predicted.

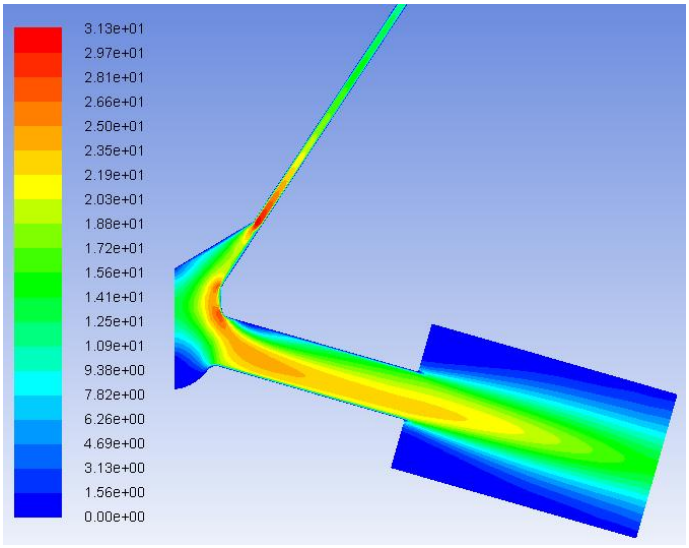

Figure .6. Velocity distribution in mid-plane of the nozzle for $\boldsymbol{h = 0.1mm}$ and $\boldsymbol{k^{0.5} = 1.094}$

Figure 7 shows formation of vapor volume fraction in different cavitation numbers. Lower cavitation numbers shows that pressure difference between inlet and outlet is not that much so vapor volume fraction forms only at the inlet of nozzle. According to figure 12a to 12f, cavitation length increases as cavitation number decreases in the nozzle. In other word, by increasing pressure difference, length of cavitation increases.

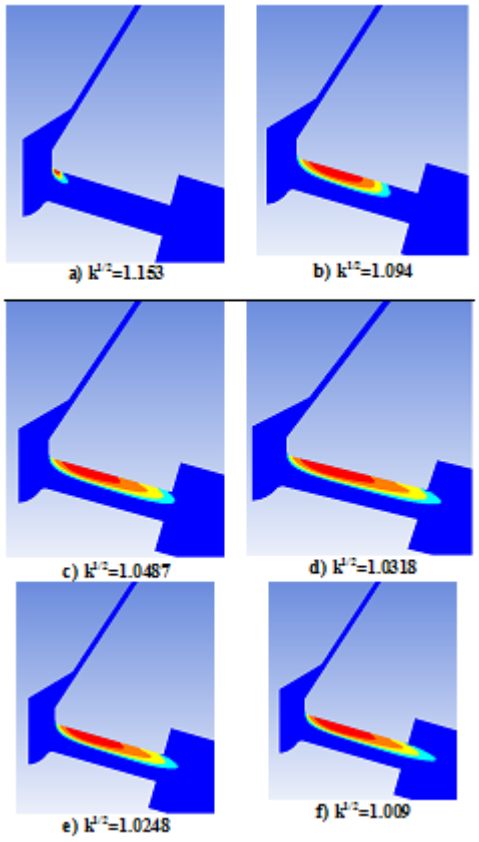

Figure.7. Distribution of vapor volume fraction when h=0.1 mm for different cavitation numbers.

As figure 8 shows, simulation of nozzle's flow for three different needle lifts was performed. When needle height is large, mass flow rate is big enough to create longitudinal cavitation (figure 8a). By decreasing needle height, length of cavitation will decrease. In the lowest amount of needle height, mass flow rate will decrease significantly which can cause cavitation to occur very slightly and it forms near needle rather

than orifice (figure 8c); In this case erosion due to bubble collapse is a probable phenomena. Figure 9 shows discharge coefficient versus square root of cavitation number in five different needle heights. According to figure 9 increasing cavitation number in a real size injector nozzle, can increase discharge coefficient at first but after increasing square root of cavitation number can no longer increase discharge coefficient. Furthermore, increasing needle height can increase discharge coefficient significantly. In most of graphs for large and small cavitation numbers, discharge coefficient is independent from cavitation number. For lower cavitation numbers, length of cavitation is big enough which occupy the whole orifice area; therefore, decreasing cavitation number in this case will not affect discharge coefficient. By decreasing cavitation number (increasing inlet pressure), discharge coefficient due to decrease in cavitation length and

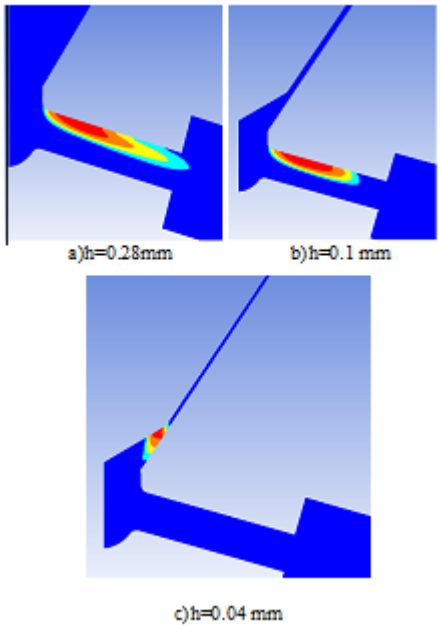

Figure. 8. Distribution of vapor volume fraction when $k^{1/2}$=1.094 for different needle lifts

width, will decrease. Hence, decreasing needle height, will decrease discharge coefficient. Effect lower needle height on discharge coefficient is more conspicuous. In needle heights which are near to minimum, since cavitation doesn't occur inside orifice, discharge coefficient changes slighter with cavitation number comparing to higher needle heights.

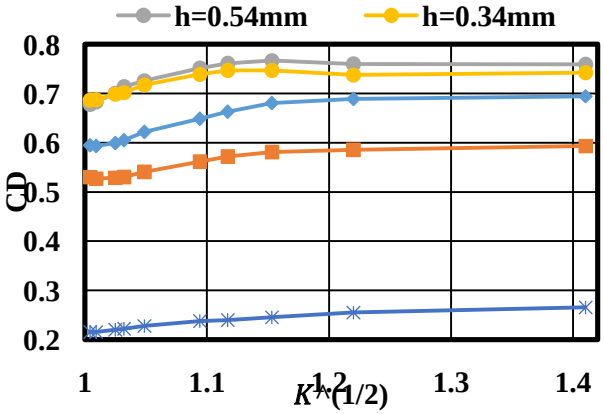

Figure.9. Discharge coefficient versus square root of cavitation number

Figure 9 shows injector nozzle geometry with different seat shapes in the middle plane. According to figure 7a, for stand nozzle orifice is located out of the needle surface region. Figure 7b shows that for improved nozzle, orifice is located at the end of the needle surface region. And finally, according to figure 7c, In VCO nozzle, orifice is is located at the beginning of the needle surface region.

5. CONCLUSION

In the present study, flow inside real-size diesel injector nozzle is investigated. Winklhofer rectangular shape nozzle is used for comparing experimental and numerical procedure that was chosen in the current study and it was found that the current setup has a good correlation with experimental results.

The following results are found in the current paper:

1- Decreasing cavitation number can increase length of vapor volume fraction which should be controlled since increasing vapor volume fraction can cause corrosion inside nozzle.

2- Decreasing needle lift can decrease length of vapor volume fraction and in the lowest amount vapor volume fraction forms at the nozzle inlet.

3- Discharge coefficient increases as cavitation number increases.

4- Increasing needle lift also increases cavitation number.

6. REFERENCES

[1]. Payri R, Molina S, Salvador FJ, Gimeno J. A study of the relation between nozzle geometry, internal flow and spray characteristics in diesel fuel injection systems. KSME Int J 2004;18(7):1222–35.

[2]. Park SH, Suh HK, Lee CS. Effect of bioethanol–biodiesel blending ratio on fuel spray behavior and atomization characteristics. Energy Fuels 2009; 23:4092–8.

[3]. Payri R, García JM, Salvador FJ, Gimeno J. Using spray momentum flux measurements to understand the influence of diesel nozzle geometry on spray characteristics. Fuel 2005;84:551–61.

[4]. Suh HK, Lee CS. Effect of cavitation in nozzle orifice on the diesel fuel atomization characteristics. Int J Heat Fluid Flow 2008; 29:1001–9.

[5]. Bermúdez V, Payri R, Salvador FJ, Gimeno J. Study of the influence of nozzle seat type on injection rate and spray behavior. Proc Inst Mech Eng D – J Automob Eng 2005; 219(D5):677–89.

[6]. Zhang J, Zhang HG, Yang K, et al. Performance analysis of regenerative organic Rankine cycle (RORC) using the pure working fluid and the zeotropic mixture over the whole operating range of a diesel engine. Energy Convers Manage 2014; 84:282–94.

[7]. Su LW, Li XR, Zhang Z, et al. Numerical analysis on the combustion and emission characteristics of forced swirl combustion system for DI diesel engines. Energy Convers Manage 2014;86:20–7.

[8]. Zheng ZQ, Yue L, Liu HF, et al. Effect of two-stage injection on combustion and emissions under high EGR rate on a diesel engine by fueling blends of diesel/gasoline, diesel/n-butanol, diesel/gasoline/n-butanol and pure diesel. Energy Convers Manage 2015; 90: 1–11.

[9]. Schmidt DP, Corradini M. The internal flow of diesel fuel injector nozzles: a review. Int J Engine Res 2001;2:1–22.

[10] Sou A, Pratama RH, Tomisaka T. Cavitation in a nozzle of fuel injector. In: 8th International symposium on cavitation, Singapore; 13–16, August 2012.

[11]. Sun ZY, Li GX, Chen C, et al. Numerical investigation on effects of nozzle's geometric parameters on the flow and cavitation characteristics within injector's nozzle for a high-pressure common-rail DI diesel engine. Energy Convers Manage 2015;89:843–61.

[12]. Wang, G., Senocak, I., Shyy, W., Ikohagi, T., Cao, S., 2001, "Dynamics of attached turbulent cavitating flows", Progress in Aerospace Sciences, vol. 37, pp. 551-581.

[13]. Senocak, I., Shyy, W., 2002, "A pressure-based method for turbulent cavitating flow computations", Journal of Computational Physics, vol. pp. 363-383.

[14]. Zeidi, S. M. J, Mahdi, M., 2015, "Evaluation of the physical forces exerted on a spherical bubble inside the nozzle in a cavitating flow with an Eulerian/Lagrangian approach", European Journal of Physics, 136(6).

[15]. Zeidi, S. M. J, Mahdi, M., 2015, "Investigation effects of injection pressure and compressibility and nozzle entry in diesel injector nozzle's flow", Journal of Applied and Computational Mechanics, 2(1), pp. 83-94. ISSN: 2383-4536.

[16]. Zeidi, S. M. J, Mahdi, M., 2014, "Effects of nozzle geometry and fuel characteristics on cavitation phenomena in injection nozzles", The 22st Annual International Conference on Mechanical Engineering-ISME2014, Tehran, Iran.

[17]. Zeidi, S. M. J, Mahdi, M., 2014, "Investigation of viscosity effect on velocity profile and cavitation formation in diesel injector nozzle", Proceedings of the 8-th International Conference on Internal Combustion Engines, Tehran, Iran.

[18]. Salvador FJ, Martínez-Lopez J, Caballer M, et al. Study of the influence of the needle lift on the internal flow and cavitation phenomenon in diesel injector nozzles by CFD using RANS methods. Energy Convers Manage 2013; 66:246–56.

[19]. Molina S, Salvador FJ, Carreres M, et al. A computational investigation on the influence of the use of elliptical orifices on the inner nozzle flow and cavitation development in diesel injector nozzles. Energy Convers Manage 2014; 79:114–27.

[20]. Wang X, Su WH. Numerical investigation on relationship between injection pressure fluctuations and unsteady cavitation processes inside high-pressure diesel nozzle holes. Fuel 2010;89:2252–9.

[21]. Sun ZY, Li GX, Yu YS, et al. Numerical investigation on transient flow and cavitation characteristic within nozzle during the oil drainage process for a high-pressure common-rail DI diesel engine. Energy Convers Manage 2015;98:507–17.

[22]. Salvador FJ, Carreres M, et al. Comparison of microsac and VCO diesel injector nozzles in terms of internal nozzle flow characteristics. Energy Convers Manage 2015;103:284–99.

[23]. Salvador FJ, Carreres M, et al. Analysis of the combined effect of hydrogrinding process and inclination angle on hydraulic performance of diesel injection nozzles. Energy Convers Manage 2015;105:1352–65.

[24]. Liu TG, Khoo BC, Xie WF. Isentropic one-fluid modelling of unsteady cavitating flow. J Comput Phys 2004;201(1):80–108.

[25]. Habchi C, Dumont N, Simonin O. Multidimensional simulation of cavitating flows in diesel injectors by a homogeneous mixture modeling approach. Atomiz Sprays 2008;18:129–62.

[26]. Peng Kärrholm F. Numerical modelling of diesel spray injection, turbulence interaction and combustion, PhD thesis, Chalmers University of Technology; 2008.

[27] Peng Kärrholm F, Weller H, Nordin N. Modelling injector flow including cavitation effects for diesel applications. In: Proceedings of FEDSM2007, 5th joint ASME/JSME fluids engineering conference, July 30–August 2, San Diego, California, USA; 2007.

[28]. T.R. Ohrn, D.W. Senser, A.H. Lefebvre, Geometrical effects on discharge coefficients for plain-orifice atomizers, Atomization Sprays 1 (2) (1991) 137–153.

[29] Kato, M., Kano, H., Date, K., Oya, T., Niizuma, K. Flow analysis in nozzle hole in consideration of cavitation. SAE Paper No.970052.

[30]. F. Payri, V. Bermudez, R. Rayri, F.J. Salvador, The influence of cavitation on the internal flow and the spray characteristics in diesel injection nozzles, Fuel 83 (2004) 419–431.

[31]. R. Payri, J.M. Garcia, F.J. Salvador, J. Gimeno, Using spray momentum flux measurements to understand the influence of diesel nozzles geometry on spray characteristics, Fuel 84 (2005) 551–561.

[32]. Par Bergstrand. The Effects of Orifice Shape on Diesel Combustion. SAE paper 2004- 01-2920.

[33]. Sibendu Som, Anita I. Ranirez, Douglas E. Longman, Suresh K. Aggarwal, Effect of nozzle orifice geometry on spray, combustion and emission characteristics under diesel engine conditions, Fuel 90 (2011) 1267–1276.

[34]. E. Winklhofer, E. Kull and E. Kelz, "Comprehensive hydraulic and flow field documentation in model throttle experiments under cavitation conditions," In: Proceedings of the ILASS-Europe conference, Zurich; 2001, pp. 574–9.

[35]. Rahmani, A., Mirmohammadi, A., Zeidi, SMJ, Shojaei, S., (2015). Numerical Approach toward Calculation of vibration Characteristics of the Multi Axles Truck Using Lagrange Method, Journal of Modern Processes in Manufacturing and Production, vol. 4(1), pp. 57-64.

[36]. Shojaei S., Zeidi SMJ., Rahmani, Mirmohammadi A., (2015). Analytical Analysis Approach to Study of the

Vibration Characteristics of the Multi Axles Truck and its Validation. Proceedings of the International Conference in New Research of Industry and Mechanical Engineering.

[37]. Zeidi, SMJ, Hoseini, P., Rahmani, A., (2017). Study of vibration specifications of a three-axle truck using Lagrange method, Journal of Modern Processes in Manufacturing and Production, vol. 6(1), pp. 83-95.

[38]. Zeidi, SMJ, Hoseini, P., Rahmani, A., (2017). Modeling a Three-axle Truck and Vibration Analysis under Sinusoidal Road Surface Excitation, International Journal of Science and Engineering Applications Volume 6 Issue 09, 2017.

[39]. Zigui Lu, Shadi Darvish, John Hardy, Jared Templeton, Jeffry Stevenson, Yu Zhong, 2017 "SrZrO3 Formation at the Interlayer/Electrolyte Interface During (La1-xSrx)1-δCo1-yFeyO3 Cathode Sintering", Journal article, The Journal of Electrochemical Society.

[40]. Darvish Shadi, Gopalan Srikanth, Zhong Yu. "Thermodynamic Stability Maps for the La0.6Sr0.4 Co0.2 Fe0.8O3±δ–CO2–O2 System for Application in Solid Oxide Fuel Cells", Journal Article, Journal of Power Sources. Published October 02, 2016.

[41]. Cheng Cheng Wang, Shuai He, Kongfa Chen, Matthew R. Rowles, Shadi Darvish, Yu Zhong and San Ping Jiang, "Effect of SO2 Poisoning on the Electrochemical Activity of La0.6 Sr0.4Co0.2Fe0.8O3-δ Cathodes of Solid Oxide Fuel Cells", Journal Article, Journal of the electrochemical Society, Published March 17, 2017.

[42]. Shadi Darvish, Yu Zhong, 2017 "Quantitative Defect Chemistry Analysis of (La1-xCax)yFeO3±δ Perovskite", Proceeding Article, 15th International Symposium on Solid Oxide Fuel Cells (SOFC-XV), The electrochemical Society.

[43]. Shadi Darvish, Surendra K. Saxena, Yu Zhong. "Quantitative Analysis of (La0.8Sr0.2)0.98MnO3±δ Electronic Conductivity Using CALPHAD Approach". Proceeding Article, the 39th International Conference on Advanced Ceramics and Composites (ICACC), Jan. 2015, John Wiley & Sons, Inc., Hoboken, NJ, USA. doi: 10.1002/ 9781119 211747.ch15.

[44]. Kadkhodapour, J. and S. Raeisi, Micro–macro investigation of deformation and failure in closed-cell aluminum foams. Computational Materials Science, 2014. 83: p. 137-148.

[45]. Hamedi, A., Hajigholizadeh, M., and Mansoori, A. 2016. Flow Simulation and Energy Loss Estimation in the Nappe Flow Regime of Stepped Spillways with Inclined Steps and End Sill: A Numerical Approach. Civil Engineering Journal. 2(9):426-437.

[46]. Hamedi, A. and Ketabdar, M. 2016. Energy Loss Estimation and Flow Simulation in the skimming flow Regime of Stepped Spillways with Inclined Steps and End Sill: A Numerical Model. International Journal of Science and Engineering Applications.5(7):399-407.

[47]. Ketabdar, M. and Hamedi, A. 2016. Intake Angle Optimization in 90-degree Converged Bends in the Presence of Floating Wooden Debris: Experimental Development. Florida Civil Engineering Journal. 2:22-27.

[48]. Ketabdar, M. 2016. Numerical and Empirical Studies on the Hydraulic Conditions of 90 degree converged Bend with Intake. International Journal of Science and Engineering Applications, 5(9), 441-444.

[49]. Hamedi, A., Malekmohammadi, I., Mansoori, A., and Roshanaei, H. 2012. Energy Dissipation in Stepped Spillway Equipped with Inclined Steps Together with End Sill. Fourth International Conference on Computational Intelligence and Communication Networks. IEEE.

[50]. Hamedi, A., Mansoori, A., Malekmohamadi, I., & Roshanaei, H. 2011. Estimating Energy Dissipation in Stepped Spillways with Reverse Inclined Steps and End Sill. In World Environmental and Water Resources Congress Reston, VA: American Society of Civil Engineers, Conference Proceeding :2528–2537.

[51]. Hamedi, A., Mansoori, A., Shamsai, A., & Amirahmadian, S. 2014. The Effect of End Sill and Stepped Slope on Stepped Spillway Energy Dissipation. Journal of Water Sciences Research, 6 :1-15.